Вісник ХНУ, серія «Фізика», вип. 29, 2018. с. 39-48

PACS: 95.30.Sf, 98.62.Sb
UDC: 530.122, 514.823, 523.163

The Analytical research of images in the gravitational lens

Semen Bronza[1], Albert Kotvytskiy[2]

[1,2] Ukrainian State University of Railway Transport
[2] V.N. Karazin Kharkov National University, Svoboda Sq. 4, Kharkov, Ukraine, 61022
bronza.sem@gmail.com[1], kotvytskiy@gmail.com[2]

ORCID: 0000-0001-8283-505X
DOI:1026565/2222-56172018-29-07

The paper researches images in point gravitational lenses by analytical methods. For research, the concept of a remote source and a remote image is introduced. It is shown that in the Schwarzschild gravitational lens, the remote source and its remote images do not differ much from each other. The following theorem is formulated and proved: the remote image of the source, in an *N*-point gravitational lens, asymptotically tends to its remote image in the Schwarzschild lens. It is shown that the images in a single-point gravitational lens are inversion conjugate.

Analytical expressions are obtained for the description of images of a circular source in the Schwarzschild lens. On this basis, the proposed classification of images of a circular source of small radius in a point lens.

Keywords: gravitational lenses; conjugate images; phases of images.

С.Д. Бронза, А.Т. Котвицький

В роботі досліджуються зображення в точкових гравітаційних лінзах аналітичними методами. Для дослідження вводяться поняття віддаленого джерела і віддаленого зображення. Показано, що в гравітаційній лінзі Шварцшильда, в картинній площині, ці два об'єкти мало відрізняються один від одного. Доведено теорему: віддалене зображення джерела, в *N*-точковій гравітаційній лінзі, асимптотичне прагне до його віддаленого зображення в лінзі Шварцшильда. Показано, що зображення в одноточковій гравітаційній лінзі інверсійно спряжені.

Отримані аналітичні вирази для опису зображень кругового джерела в лінзі Шварцшильда. На цій основі запропоновано класифікацію зображень кругового джерела малого радіусу.

Ключові слова: гравітаційні лінзи, спряжені зображення, фази зображень.

С.Д. Бронза, А.Т. Котвицкий

В работе исследуются изображения в точечных гравитационных линзах аналитическими методами. Для исследования вводятся понятие удаленного источника и удаленного изображения. Показано, что в гравитационной линзе Шварцшильда, в картинной плоскости, эти два объекта мало отличаются друг от друга. Доказана теорема: удаленное изображение источника, в *N*-точечной гравитационной линзе, асимптотически стремится к его удаленному изображению в линзе Шварцшильда. Показано, что изображения в одноточечной гравитационной линзе инверсионно сопряжены.

Получены аналитические выражения для описания изображений кругового источника в линзе Шварцшильда. На этой основе предложена классификация изображений кругового источника малого радиуса.

Ключевые слова: гравитационные линзы, сопряженные изображения, фазы изображений.

Physical formulation of the problem

Let R^2_X and R^2_Y be vector spaces. It is known, [1], [2], that N - point gravitational lens sets a unique map

$$L : (R^2_X \setminus \Lambda) \to R^2_Y , \tag{1}$$

were $\Lambda = \{ l_i \,|\, i = 1,2,...,N \}$ - set of radius - vectors $\vec{l}_i$ point masses.

The mapping L is uniquely definitely a vector equation

$$\vec{y} = \vec{x} - \sum_i m_i \frac{\vec{x} - \vec{l}_i}{\left| \vec{x} - \vec{l}_i \right|^2}, \tag{2}$$

where, for dimensionless point masses m_i, the ratio $\sum_i m_i = 1$ is valid.

We add the vector spaces R^2_X and R^2_Y to affine ones.We will define orthonormal bases in them. For the unit of rationing, we take the Einstein - Chvolson radius. The resulting affine spaces R^2_X and R^2_Y are called the lens plane and the source plane, respectively. For some researches, they are combined and called the picture plane [9,10].

The mapping L^{-1} inverse to (1), in general, is multivalued.

$$L^{-1}: R^2_Y \to (R^2_X \setminus \Lambda). \tag{3}$$

It can, naturally, be continued from $\left(R^2_X \setminus \Lambda\right)$ to all R^2_X (we will leave the same notation behind the continued mapping), i.e.

$$L^{-1}: R^2_Y \to R^2_X. \tag{4}$$

Some authors call mapping (4) as a lens mapping, see, for example, [3].

The mapping L can be written in the coordinate form :

$$\begin{cases} y_1 = x_1 - \sum\limits_{i=1}^{N} m_i \frac{x_1 - a_i}{(x_1-a_i)^2+(x_2-b_i)^2} \\ y_2 = x_2 - \sum\limits_{i=1}^{N} m_i \frac{x_2 - b_i}{(x_1-a_i)^2+(x_2-b_i)^2} \end{cases}, \tag{5}$$

were $\bar{x} = (x_1, x_2)$, $\bar{y} = (y_1, y_2)$, $\bar{l}_i = (a_i, b_i)$, and m_i normalized, dimensionless point masses satisfying the relation $\sum m_i = 1$.

A special case of the N – point gravitational lens is the Schwarzschild lens [3], [4], which is determined by the condition $N=1$, $a_1=0$, $b_1=0$, and $m=1$.

$$\begin{cases} y_1 = x_1 - \dfrac{x_1}{x_1^2 + x_2^2} \\ y_2 = x_2 - \dfrac{x_2}{x_1^2 + x_2^2} \end{cases}. \tag{6}$$

The Asymptotic behaviour of the map L

One of the main tasks of the theory of gravitational lensing is the problem of constructing images from a given source (direct problem).

In this paper, we assume that the S source is uniform and flat.

In topological terms, the source is:

- connected area;
- of course - connected area;
- the region boundary consists of a finite number of arcs of smooth curves [5, 6].

The source image, in topological terms, is also an area. In general, a source image consists of several connected components.

The diameter of the S source is called the diameter of the minimum circle to which it belongs, and the center of the source S is the center O_S of this circle. We say that the source of S is small, if its diameter d_S is significantly less than the unit $d_S << 1$, and deleted (located far away) if the module $|\vec{O}_S|$ of the radius-vector $\vec{O}_S$ is significantly greater than one, i.e. $|\vec{O}_S| >> 1$. Similarly, we define the concept: the diameter and canter of the connected components of the image, and the remote image.

Occurs

Theorem 1. Let the source S and its images be viewed in the picture plane. If the source is small and deleted, then its image has:

- remote component of connectivity S_1, such that $|O_{S_1}| > |O_S|$;
- each point S_1, with $|O_S| \to \infty$, tends to its image in S_1;
- restriction of the mapping L to S_1 is a bijection of S_1 to S.

First we prove the lemma

Lemma 2. The remote image of a remote point source in N-point gravitational lens tends to its remote image in the Schwarzschild lens.

Proof. Let points $(a_i, b_i) \in R^2_X$ and $\delta = \sqrt{x_1^2 + x_2^2}$. Let $\delta \to \infty$. Where we have:

$$x_1 - \sum_{i=1}^{N} m_i \frac{x_1 - a_i}{(x_1-a_i)^2+(x_2-b_i)^2} = x_1 - \frac{x_1}{x_1^2 + x_2^2} + o(\delta).$$

A similar relation holds for the right side of the second equation of system (5).

For system (5), with $\delta \to \infty$, we have:

$$\begin{cases} y_1 = x_1 - \sum_{i=1}^{N} m_i \frac{x_1 - a_i}{(x_1 - a_i)^2 + (x_2 - b_i)^2} \\ y_2 = x_2 - \sum_{i=1}^{N} m_i \frac{x_2 - b_i}{(x_1 - a_i)^2 + (x_2 - b_i)^2} \end{cases} \Rightarrow \begin{cases} y_1 = x_1 - \frac{x_1}{x_1^2 + x_2^2} \\ y_2 = x_2 - \frac{x_2}{x_1^2 + x_2^2} \end{cases}. \quad (10)$$

Thus, when the image is removed from the origin of coordinates in an *N*-point lens, it differs little from the images in the Schwarzschild lens. But for the Schwarzschild lens, it is known that the points of the remote source are close to the points of the remote component of the image.

Indeed, if $y_1^2 + y_2^2 \to \infty$, then:

$$x = \frac{1}{2}\left(y_1 \pm y_1 \sqrt{1 + \frac{4}{y_1^2 + y_2^2}} \right) \to x_1 = \begin{cases} y_1 \\ 0 \end{cases}, \quad (11)$$

thus, the abscissa S_1 tends to abscissa *S*. The same is true for ordinates.

The proof is complete.

Proof of Theorem 1

We show that the points of the S_1 (the remote component of the image of the source of the *S* in the Schwarzschild lens) tend to their images, if $|O_S| \to \infty$. For the Schwarzschild lens we have: $\sqrt{(x_1 - y_1)^2 + (x_2 - y_2)^2} = 1/\sqrt{x_1^2 + x_2^2} = 1/\delta$. In addition, from $|O_S| \to \infty \Rightarrow r \to \infty$, and therefore $\sqrt{(x_1 - y_1)^2 + (x_2 - y_2)^2} = 1/\delta \to 0$.

The restriction of the mapping *L* to S_1 is a bijection of S_1 to *S*. Indeed, a point from *S* has two pre-images, one of which belongs to the remote image S_1, and the second is in the unit circle. Considering the lemma, we have: the assertions of Theorem 1 are true.

Images of a circular source in the Schwarzschild lens

It is known that each point source located not at the origin of coordinates has two points (further conjugate) images in the Schwarzschild lens, one of which is in the unit circle and the other outside it.

Occurs

Theorem 2. If g_1, g_2 is the coordinates of one of the conjugate images in the Schwarzschild lens, then the coordinates of the second image are $-g_1\left(g_1^2 + g_2^2\right)^{-1}, -g_2\left(g_1^2 + g_2^2\right)^{-1}$.

Proof. Because

$$\begin{cases} y_1 = y_1(x_1, x_2) = x_1 - \frac{x_1}{x_1^2 + x_2^2} \\ y_2 = y_2(x_1, x_2) = x_2 - \frac{x_2}{x_1^2 + x_2^2} \end{cases},$$

we directly verify that:

$$\begin{cases} y_1(x_1, x_2) \equiv y_1\left(-\frac{x_1}{x_1^2 + x_2^2}, -\frac{x_2}{x_1^2 + x_2^2} \right) \\ y_2(x_1, x_2) \equiv y_2\left(-\frac{x_1}{x_1^2 + x_2^2}, -\frac{x_2}{x_1^2 + x_2^2} \right) \end{cases}, \quad (12)$$

From (12) it follows: both images have the same prototype (source).

The theorem is proved.

Corollary of Theorem 2

Any small one connected source that does not contain the origin has two images in the Schwarzschild lens.

The points of these two images are conjugate and their coordinates satisfy Theorem 2.

We will call such images conjugated.

Let the source be a $D_\varepsilon = D_\varepsilon(a)$ disk of radius ε with canter at point $(a, 0)$ and its boundary ∂D_ε is determined by a parametric equation:

$$\begin{cases} y_1 = t \\ y_2 = \pm\sqrt{\varepsilon^2 - (t_1 - a)^2} \end{cases}. \tag{13}$$

We substitute (13) into the system of equations (6), we have:

$$\begin{cases} t = x_1 - \dfrac{x_1}{x_1^2 + x_2^2} \\ \pm\sqrt{\varepsilon^2 - (t-a)^2} = x_2 - \dfrac{x_2}{x_1^2 + x_2^2} \end{cases}. \tag{14}$$

We exclude t from system (14) we get:

$$\left(x_1^2 + x_2^2 - 1\right)^2 - 2ax_1\left(x_1^2 + x_2^2 - 1\right) + (a^2 - \varepsilon^2)(x_1^2 + x_2^2) = 0. \tag{15}$$

Let's move in the plane of the lens from the Cartesian x_1, x_2 coordinates to the polar coordinates of the r, ϕ:

$$\begin{cases} x_1 = r\cos\phi \\ x_2 = r\sin\phi \end{cases}, \tag{16}$$

we have:

$$\left(r^2 - 1\right)^2 - 2a\left(r^2 - 1\right)r\cos\phi + (a^2 - \varepsilon^2)r^2 = 0. \tag{17}$$

We research the equation (15) and (17), for this we consider some special cases:

a) $a = 0$; b) $|a| = \varepsilon$; c) $|a| < \varepsilon$; d) $|a| > \varepsilon$.

Case a). From equation (18) (17) we get two solutions that have a physical meaning:

$$r_{1,2} = \frac{\pm\varepsilon + \sqrt{\varepsilon^2 + 4}}{2}. \tag{18}$$

From (17) we have: the image of the disk D_ε under the mapping L^{-1} is the ring k_ε.

The ring is formed by circles:

$$r_1 = \frac{\sqrt{\varepsilon^2 + 4} + \varepsilon}{2}, \quad r_2 = \frac{\sqrt{\varepsilon^2 + 4} - \varepsilon}{2}. \tag{19}$$

The radii of the circles are reciprocal, i.e. $r_1 = 1/r_2$.

The unit circle divides the ring into two rings. Rings are conjugated. (see Fig.1.).

The ring has a thickness of $d = \varepsilon$, really:

$$d = r_1 - r_2 = \frac{\sqrt{\varepsilon^2 + 4} + \varepsilon}{2} - \frac{\sqrt{\varepsilon^2 + 4} - \varepsilon}{2} = \varepsilon. \tag{20}$$

The middle line of a k_ε ring is a circle of radius $r = \dfrac{\sqrt{\varepsilon^2 + 4}}{2}$.

The area of the ring k_ε is equal to:

$$S_\varepsilon = \pi\varepsilon\sqrt{\varepsilon^2 + 4}. \tag{21}$$

Case b).

If $|a| = \varepsilon \Rightarrow a = \pm\varepsilon$. Consider the case of $a = \varepsilon$.

We substitute $a = \varepsilon$ into (15). We have: the equation is divided into two:

$$\left(x_1^2 + x_2^2 - 1 - 2\varepsilon x_1\right)\left(1 - \frac{1}{x_1^2 + x_2^2}\right) = 0. \tag{22}$$

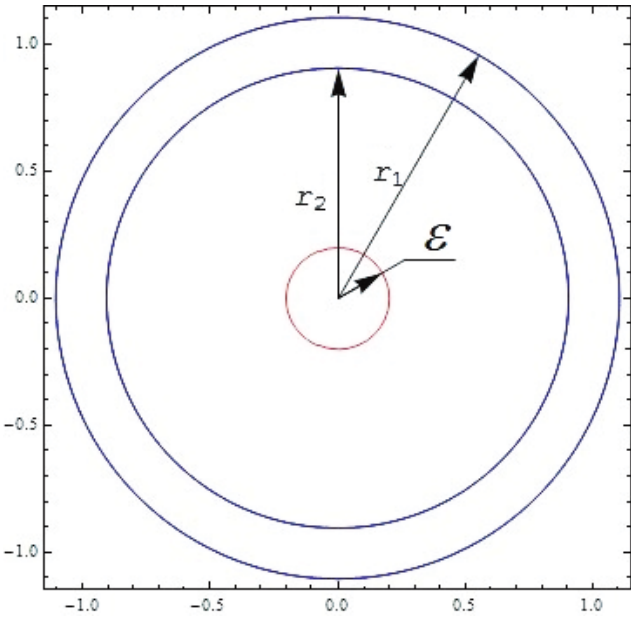

Fig.1. The boundary of the ring k_ε is defined by circles with radii of $r_{1,2}$. The ring k_ε is an image of the D_ε disk. The radius ε of the D_ε disk is equal to *0,2* from the radius of Einstein - Chvolson.

From equation (22) we get two solutions:

$$x_1^2 + x_2^2 = 1, \tag{23}$$

$$(x_1 - \varepsilon)^2 + x_2^2 = 1 + \varepsilon^2. \tag{24}$$

Equations (23) and (24) are equations of circles.

Therefore, the image of the D_ε disk, when displaying L^{-1}, will be two circular wells *I* and *II*.

The wells are formed by circles (23,24), are conjugate.

Circles intersect at points A_1 *(0,1)* and A_2 *(0,-1)*.

The thickness of the left well is $h_1 = 1 + \varepsilon - \sqrt{1+\varepsilon^2}$.

The thickness of the right well is $h_2 = \varepsilon + \sqrt{1+\varepsilon^2} - 1$.

$$S_1 = \frac{\pi}{2} + \int_{-1}^{1} \left(\varepsilon - \sqrt{1 + \varepsilon^2 - x_2^2} \right) dx_2 = \\ = \frac{\pi}{2} + \varepsilon - (1+\varepsilon^2) arcctg\,\varepsilon \tag{25}$$

The area of the left well is:

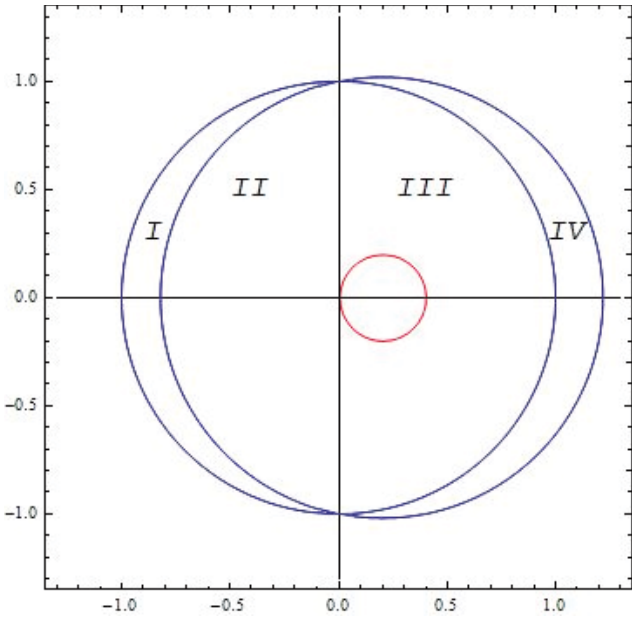

Fig.2. The source radius is ε*=0,2* of the Einstein-Chvolson radius. The area of the left well is $S_I = S_{I,II} - S_{II}$, the area of the right well $S_{IV} = S_{II,III,IV} - S_{II} - S_{III}$.

$$S_2 = \pi(1+\varepsilon^2) + \int_{-1}^{1} \left(\varepsilon - \sqrt{1 + \varepsilon^2 - x_2^2} \right) dx_2 - \frac{\pi}{2}. \\ = \frac{\pi}{2} + \pi\varepsilon^2 + \varepsilon - (1+\varepsilon^2) arcctg\,\varepsilon \tag{26}$$

The area of the right hole is equal to:

$$S = S_1 + S_2 = \pi + \pi\varepsilon^2 + 2\varepsilon - 2(1+\varepsilon^2) \cdot arctg\,\varepsilon. \tag{27}$$

Similarly, we consider the case of $a = -\varepsilon$.

Due to the obvious symmetry, the sum of the *S* - areas of the wells and in this case can be calculated by the formula (27).

Case c) $|a| < \varepsilon$.

The value of the polar radius $r \geq 0$.

From equation (17) we get:

$$r = \frac{1}{2}\left(\left(a\cos\phi \pm \sqrt{\varepsilon^2 - a^2 \sin^2\phi} \right) + \sqrt{\left(a\cos\phi \pm \sqrt{\varepsilon^2 - a^2 \sin^2\phi} \right)^2 + 4} \right). \tag{28}$$

If $a < \varepsilon$, then the curve (28):

- consists of two ovals (closed Jordan curves) that are not circles;
- ovals are one in another;
- ovals are the boundary of a doubly connected domain homeomorphic to a ring.

Inner oval:

$$r_1 = \frac{1}{2}\left(a\cos\varphi - \sqrt{\varepsilon^2 - a^2 \sin^2\varphi} + \sqrt{\left(a\cos\varphi - \sqrt{\varepsilon^2 - a^2 \sin^2\varphi} \right)^2 + 4} \right). \tag{29}$$

Outside oval:

$$r_2 = \frac{1}{2}\left(a\cos\varphi + \sqrt{\varepsilon^2 - a^2 \sin^2\varphi} + \sqrt{\left(a\cos\varphi + \sqrt{\varepsilon^2 - a^2 \sin^2\varphi} \right)^2 + 4} \right). \tag{30}$$

The area of a two connected region homeomorphic to a ring is:

$$S = S_2 - S_1 = \frac{1}{2}\int_0^{2\pi} r_2{}^2 d\varphi - \frac{1}{2}\int_0^{2\pi} r_1{}^2 d\varphi = \frac{1}{2}\int_0^{2\pi} (r_2{}^2 - r_1{}^2) d\varphi = \frac{1}{2}\int_0^{2\pi} (r_2 - r_1)(r_2 + r_1) d\varphi, \tag{31}$$

where

$$\begin{aligned}(r_2 - r_1)(r_2 + r_1) &= 2a\cos\varphi\sqrt{\varepsilon^2 - a^2\sin^2\varphi} + \\ &+ \frac{1}{2}\left(\sqrt{\varepsilon^2 - a^2\sin^2\varphi} + a\cos\varphi\right)\sqrt{a^2\cos 2\varphi + \varepsilon^2 + 2a\cos\varphi\sqrt{\varepsilon^2 - a^2\sin^2\varphi} + 4} + \\ &+ \frac{1}{2}\left(\sqrt{\varepsilon^2 - a^2\sin^2\varphi} - a\cos\varphi\right)\sqrt{a^2\cos 2\varphi + \varepsilon^2 - 2a\cos\varphi\sqrt{\varepsilon^2 - a^2\sin^2\varphi} + 4}\end{aligned}. \tag{32}$$

The two connected regions are symmetric about the polar axis. The function under the integral sign is even and 2π is periodic. For the area of the area we have:

$$S = \int_0^{\pi} (r_2 - r_1)(r_2 + r_1) d\varphi \cdot$$

The integral (31) is an elliptic integral.

Comment. Expression (31) with a value of $a = 0$ reduces to equation (21).

Case d). $|a| > \varepsilon$. If $a > \varepsilon$, then the curve:

- consists of two ovals (closed Jordan curves) that are not circles;
- ovals are one outside the other;
- each oval is the boundary of one connected region of a homeomorphic disk.

The functions $r_1 = r_1(\varphi)$ and $r_2 = r_2(\varphi)$ are defined if $\varepsilon^2 - a^2\sin^2\varphi \geq 0$.

Where do we get:

$$-\arcsin\frac{\varepsilon}{|a|} \leq \varphi \leq \arcsin\frac{\varepsilon}{|a|} \text{ and } \pi - \arcsin\frac{\varepsilon}{|a|} \leq \varphi \leq \pi + \arcsin\frac{\varepsilon}{|a|} \cdot \tag{33}$$

The ovals in the right and left half-planes are determined by equation (28) under condition (33).

If $a > 0$, we have.

The far arc of the right oval is determined by expression (30) and the condition $-\arcsin\frac{\varepsilon}{a} \leq \phi \leq \arcsin\frac{\varepsilon}{a}$.

The near arc of the right oval is determined by expression (29) and the condition $-\arcsin\frac{\varepsilon}{a} \leq \phi \leq \arcsin\frac{\varepsilon}{a}$

The far arc of the left oval (the arc is conjugated with the far arc of the right oval) is determined by expression (30) and the condition $\pi - \arcsin\frac{\varepsilon}{a} \leq \phi \leq \pi + \arcsin\frac{\varepsilon}{a}$.

The near arc of the left oval (the arc is conjugated with the near arc of the right oval) is determined by expression (29) and the condition $\pi - \arcsin\frac{\varepsilon}{a} \leq \phi \leq \pi + \arcsin\frac{\varepsilon}{a}$.

The right oval limits one connected area. The square of this area is equal to:

$$S = S_2 - S_1 = \frac{1}{2}\int_{\pi-\arcsin\frac{\varepsilon}{a}}^{\pi+\arcsin\frac{\varepsilon}{a}} r_2{}^2 d\varphi - \frac{1}{2}\int_{\pi-\arcsin\frac{\varepsilon}{a}}^{\pi+\arcsin\frac{\varepsilon}{a}} r_1{}^2 d\varphi = \frac{1}{2}\int_{\pi-\arcsin\frac{\varepsilon}{a}}^{\pi+\arcsin\frac{\varepsilon}{a}} (r_2{}^2 - r_1{}^2) d\varphi = \frac{1}{2}\int_{\pi-\arcsin\frac{\varepsilon}{a}}^{\pi+\arcsin\frac{\varepsilon}{a}} (r_2 - r_1)(r_2 + r_1) d\varphi,$$

where the integrand is defined by equation (32).

Similarly, we can calculate the area of a region that is bounded by the left oval.

Classification of circular source images in 1-point gravitational lens

Assume without loss of generality, that the circular source center is on abscissa and source radius is small. For images of circular source in 1-point gravitational lens, we have classification

Theorem 3. Images of circular source in 1-point gravitational lens belong to only one of the following sets (we call set as phase, we show circular source and images of circular source on the picture plane)

- phase «-7» of intersection with image on the left (center of circular image is on abscissa far left of the origin of the coordinate system, circular image intersects with its left image);
- phase «-6» of touching with image on the left (center of circular source is on abscissa far left of the origin, circular source touches its left image);
- phase «-5» of 1-connected convex images (center of circular source is on abscissa on the left of the origin of the coordinate system, circular source has two 1-connected images, source is located between them and does not intersect them, each image is convex)
- phase «-4» of 1-connected special transition images (center of circular source is left of the origin on abscissa, circular source has two 1-connected images, source is located between them and does not intersect them, each image become nonconvex);
- phase «-3» of 1-connected nonconvex images (center of circular source is left of the origin on abscissa, circular source has two 1-connected images, source is located between them and does not intersect them, each image is nonconvex);
- phase «-2» circular alveolus (center of circular source is left of the origin on abscissa, touches origin, circular source has two 1-connected images, that is circular alveolus, that is formed by two circles, source is located inside circles);
- phase «-1» «left Einstein ring» (center of circular source is left of the origin on abscissa, the origin belongs to the circular source, image of circular source is 2-connected region, region boundary is disjoint closed Jordan arc, source is located inside 2-connected region);
- phase «0» «Einstein ring» (center of circular source is at the origin, image of circular source is a circle that is formed by two coaxial circles with centers at the origin);
- phase «1» «right Einstein ring» (symmetrical image of phase «-1» relative to ordinate axes);
- phase «2» (symmetrical image of phase «-2» relative to ordinate axes);
- phase «3» (symmetrical image of phase «-3» relative to ordinate axes);
- phase «4» (symmetrical image of phase «-4» relative to ordinate axes);
- phase «5» (symmetrical image of phase «-5» relative to ordinate axes);
- phase «6» (symmetrical image of phase «-6» relative to ordinate axes);
- phase «7» (symmetrical image of phase «-7» relative to ordinate axes);

We illustrate Theorem 3 in Fig.3 in appendix.

Remark. Each phase is totally defined by values of two parameters: coordinates of circular source center *(a,0)* and its radius ε.

Parameters defines phases as follows: phase «-7»: $a < \varepsilon - \frac{1}{2\varepsilon}$ Fig.3.n; phase «-6»: $a = \varepsilon - \frac{1}{2\varepsilon}$ Fig.3.l; phase «-5»: $\varepsilon - \frac{1}{2\varepsilon} < a < -1 + \varepsilon$ Fig.3.j; phase «-4»: $a = -1 + \varepsilon$ Fig.3.h; phase «-3»: $-1 + \varepsilon < a < -\varepsilon$ Fig.3.f; phase «-2»: $a = -\varepsilon$ Fig.3.d; phase «-1»: $-\varepsilon < a < 0$ Fig.3.b; phase «0»: $a = 0$ Fig.3.a; phase «1»: $0 < a < \varepsilon$ Fig.3.c; phase «2»: $a = \varepsilon$ Fig.3.e; phase «3»: $\varepsilon < a < 1 - \varepsilon$ Fig.3.g; phase «4»: $a = 1 - \varepsilon$ Fig.3.i; phase «5»: $1 - \varepsilon < a < \frac{1}{2\varepsilon} - \varepsilon$ Fig.3.k; phase «6»: $a = \frac{1}{2\varepsilon} - \varepsilon$ Fig.3.m; phase «7»: $a > \frac{1}{2\varepsilon} - \varepsilon$ Fig.3.o.

Corollary. The phase classification in Theorem 3 is linear; it contains 15 phases including 7 point and 8 interval phases. Classification is symmetrical relative central phase – Einstein ring. Each phase is totally defined by values of two parameters: coordinates of circular source center *(a,0)* and its radius ε, they are invariants.

Acknowledgements

Albert Kotvytskiy thanks for support SFFR, Ukraine, Project No. 32367.

Appendix

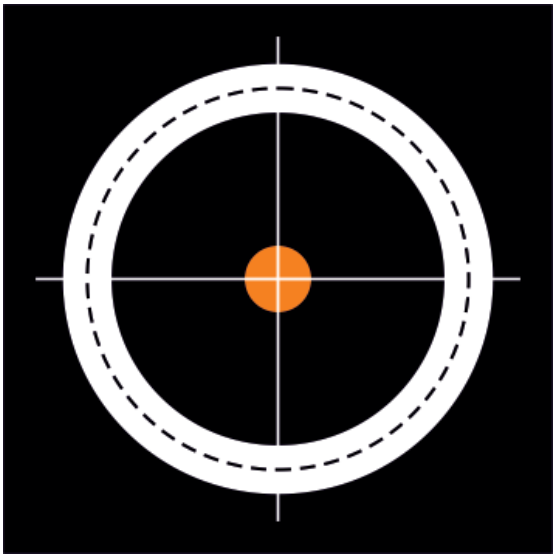

Fig.3.a. Phase «0» *a=0.*

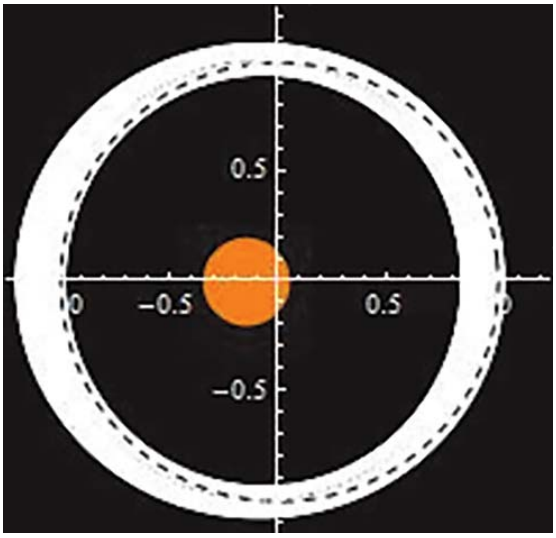

Fig.3.b. Phase «-1» $-\varepsilon < a < 0$.

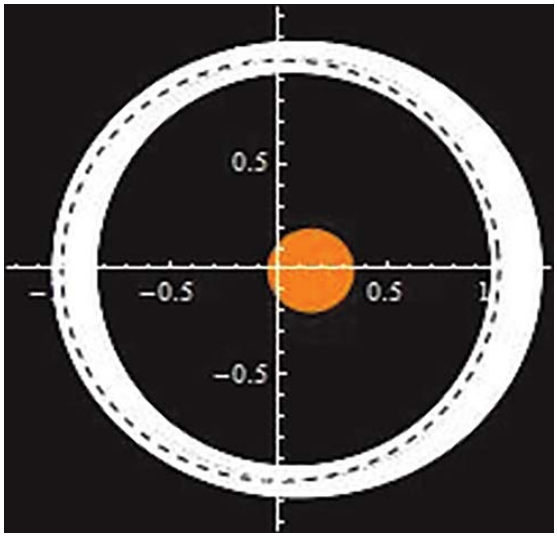

Fig.3.c. Phase «1» $0 < a < \varepsilon$.

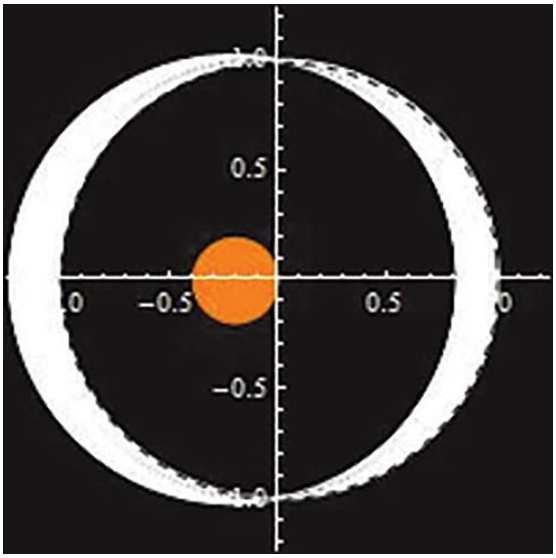

Fig.3.d. Phase «-2» $a = -\varepsilon$.

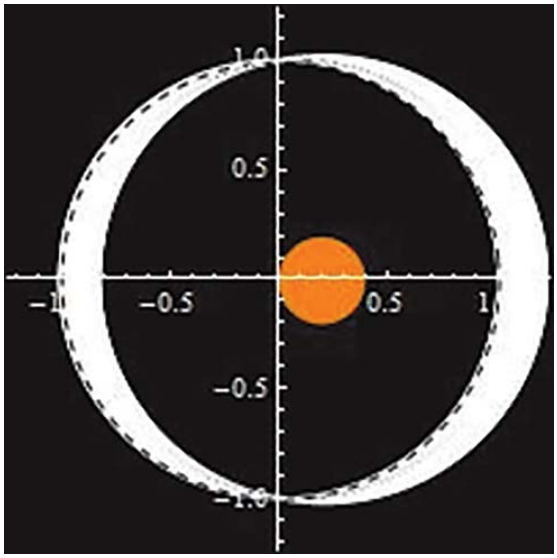

Fig.3.e. Phase «2» $a = \varepsilon$.

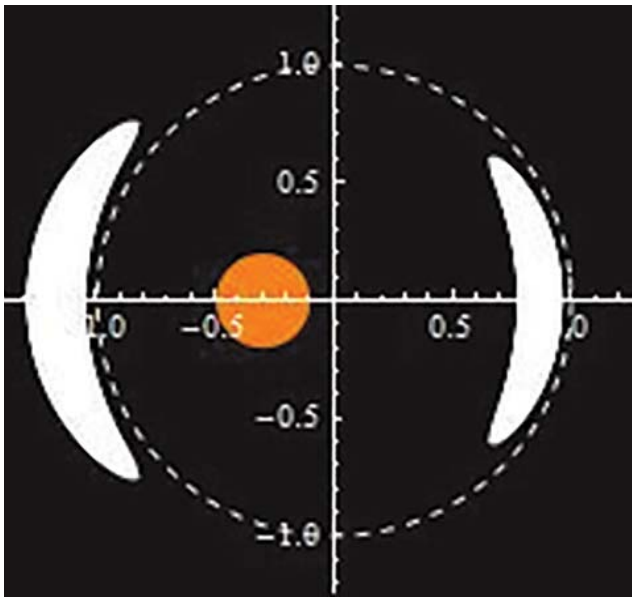

Fig.3.f. Phase «-3» $-1+\varepsilon < a < -\varepsilon$.

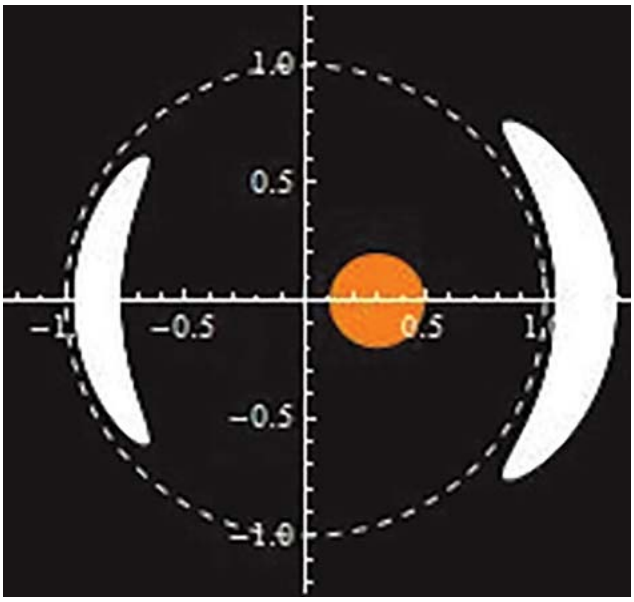

Fig.3.g. Phase «3» $\varepsilon < a < 1-\varepsilon$.

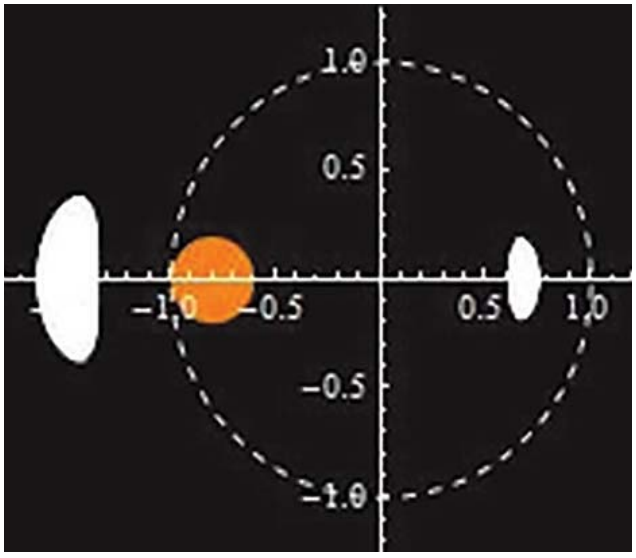

Fig.3.f. Phase «-4» $a = -1+\varepsilon$.

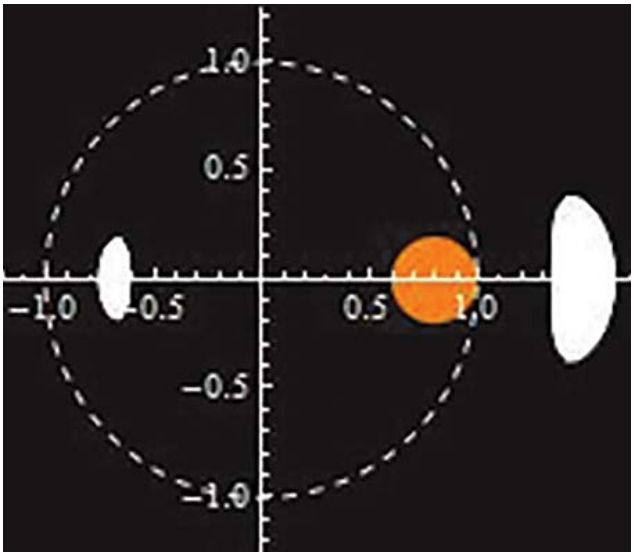

Fig.3.g. Phase «4» $a = 1-\varepsilon$.

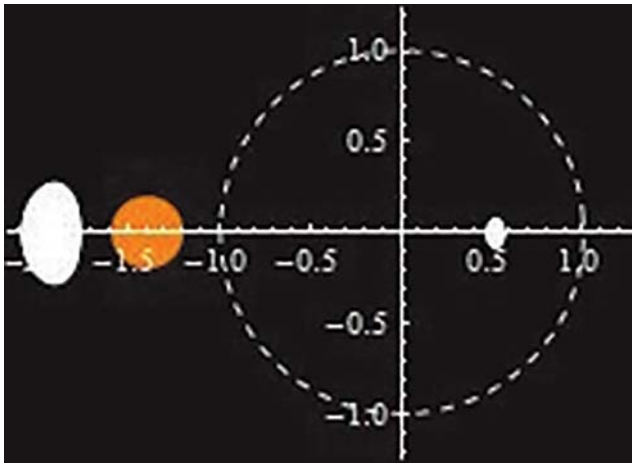

Fig.3.j. Phase «-5» $\varepsilon - \frac{1}{2\varepsilon} < a < -1+\varepsilon$.

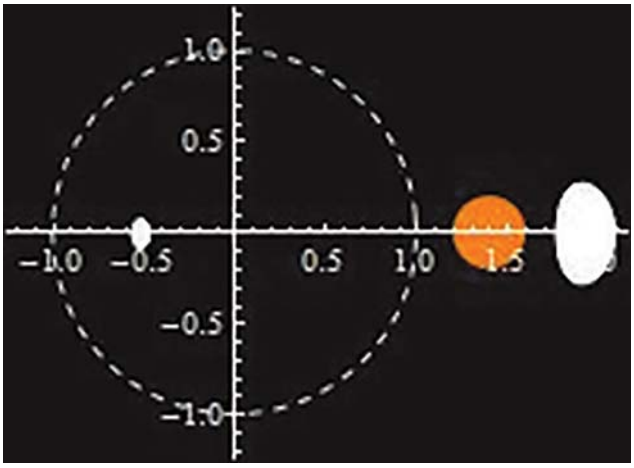

Fig.3.k. Phase «5» $1-\varepsilon < a < \frac{1}{2\varepsilon} - \varepsilon$.

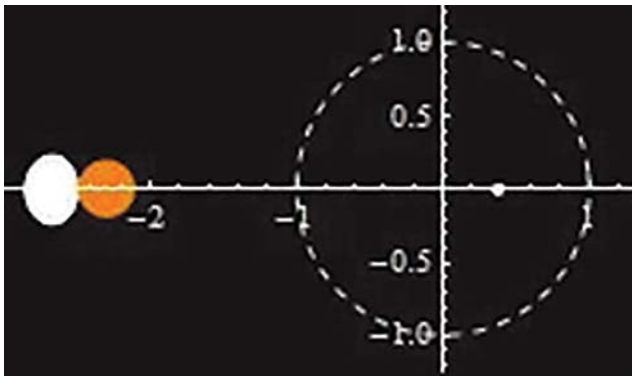

Fig.3.l. Phase «-6» $a = \varepsilon - \frac{1}{2\varepsilon}$.

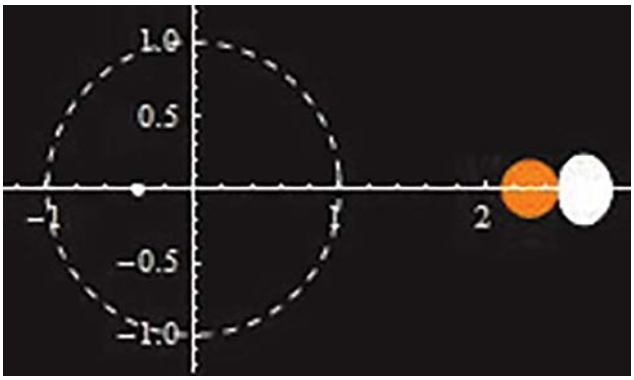

Fig.3.m. Phase «6» $a = \frac{1}{2\varepsilon} - \varepsilon$.

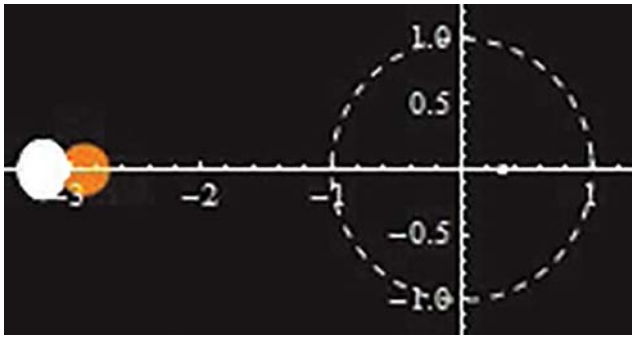

Fig.3.n. Phase «-7» $a < \varepsilon - \frac{1}{2\varepsilon}$.

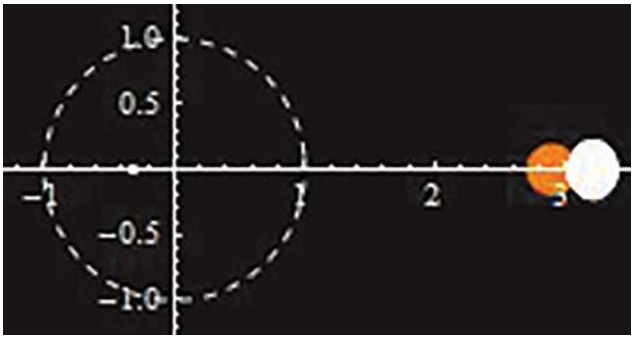

Fig.3.o. Phase «7» $a > \frac{1}{2\varepsilon} - \varepsilon$.

The source is presented in the form of a yellow disc. Images are presented as white areas. The dashed circle is the Einstein ring.

References

1. Bronza S.D., Kotvytskiy A.T. Bulletin of Kharkiv Karazin National University “Physics”, V.26. (2017) P.6-32.
2. Albert T. Kotvytskiy, Semen D. Bronza, Volodymyr Yu. Shablenko Acta Polytechnica 57(6), (2017) P.404–411. (doi:10.14311/AP.2017.57.0404)
3. Schneider P., Ehlers J., Falco E.E. Gravitational lenses. Springer-Verlag Berlin Heidelberg 1999 P. 560.
4. Steven Weinberg Cosmology OXFORD university press, 2008. P 593.
5. Lavrentiev M.A., Shabat B.V., Metody teorii funciy kompleksnogo peremennogo (Moscow), 1973 P. 716. (in Russian)
6. Gurvits A. Kurant R., Teorija funkciy (Moscow), 1968 P. 648. (in Russian)
7. Kotvytskiy A.T., Bronza S.D. Odessa Astronomical Publications, vol. 29 (2016), P.31-33. (DOI: 10.18524/1810-4215.2016.29.84958)
8. A.T. Kotvytskiy, S.D. Bronza, S.R. Vovk Bulletin of Kharkiv Karazin National University “Physics”, V.24. (2016) P.55-59 (arXiv:1809.05392)
9. A. Kotvytskiy, S. Bronza, V. Shablenko, K. Nerushenko Збірник наукових праць, Вінниця (2017) p. 198-213.
10. A. T. Kotvytskiy, S. D. Bronza, V. Y. Shablenko. Odessa Astronomical Publications, vol. 30 (2017), P.35-37.